Science of the Total Environment 893 (2023) 164614

Contents lists available at ScienceDirect

Science of the Total Environment

journal homepage: www.elsevier.com/locate/scitotenv

Nitrogen from agriculture and temperature as the major drivers of deoxygenation in the central Bohai Sea

Fuxia Yang [a,b,c], Hao Wang [d], Alexander F. Bouwman [c,e,*], Arthur H.W. Beusen [c,e], Xiaochen Liu [c], Junjie Wang [c], Zhigang Yu [a,b,f], Qingzhen Yao [a,b,f,**]

[a] Frontiers Science Center for Deep Ocean Multispheres and Earth System, Key Laboratory of Marine Chemistry Theory and Technology, Ministry of Education, Ocean University of China, Qingdao 266100, China
[b] College of Chemistry and Chemical Engineering, Ocean University of China, 238 Songling Road, Qingdao 266100, China
[c] Department of Earth Sciences, Faculty of Geosciences, Utrecht University, 3584 CB Utrecht, the Netherlands
[d] Deltares, 2600 MH Delft, the Netherlands
[e] PBL Netherlands Environmental Assessment Agency, 2500 GH The Hague, the Netherlands
[f] Laboratory of Marine Ecology and Environmental Science, Laoshan Laboratory, Qingdao 266071, China

HIGHLIGHTS

- Agriculture contributes 72 % to river N export for Bohai Sea.
- Water-column oxygen consumption increased by 20 % during 1980–2010.
- Nitrogen from agriculture and temperature are the main drivers of deoxygenation.
- Even in a sustainable scenario SSP1, deoxygenation will still well above 1980 levels.

GRAPHICAL ABSTRACT

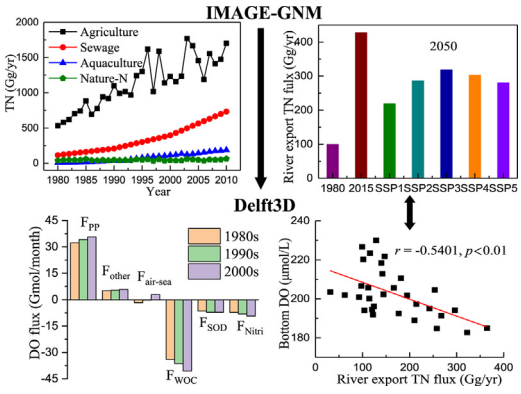

ARTICLE INFO

Guest Editor: Estela Romero

Keywords:
Deoxygenation
Agricultural nitrogen loss
Eutrophication
Sediment oxygen demand
Bohai Sea
Water-column oxygen consumption

ABSTRACT

Agricultural N losses strongly dominate the N delivery (average 72 % of total N delivery to rivers in the period 1980–2010) in the rivers discharging into the Bohai Sea, a semi-enclosed marginal sea, which has been suffering from eutrophication and deoxygenation since the 1980s. In this paper we investigate the relationship between N loading and deoxygenation in the Bohai Sea, and consequences of future N loading scenarios. Using modeling for the period 1980–2010, the contributions of different oxygen consumption processes were quantified and the main controlling mechanisms of summer bottom dissolved oxygen (DO) evolution in the central Bohai Sea were determined. Model results show that the water column stratification during summer impeded the DO exchange between oxygenated surface water and oxygen-poor bottom water. Water column oxygen consumption (60 % of total oxygen consumption) was strongly correlated with elevated nutrient loading, while nutrient imbalances (increasing N:P ratios) enhanced harmful algal bloom proliferation. Future scenarios show that deoxygenation may be reduced in all scenarios owing to increasing agricultural efficiency, manure recycling and wastewater treatment. However, even in the sustainable development scenario SSP1, nutrient discharges in 2050 will still exceed the 1980 levels, and with further enhancement of water stratification due to climate warming, the risk of summer hypoxia in bottom waters may persist in the coming decades.

* Correspondence to: A.F. Bouwman, Department of Earth Sciences, Faculty of Geosciences, Utrecht University, 3584 CB Utrecht, the Netherlands.
** Correspondence to: Q. Yao, Frontiers Science Center for Deep Ocean Multispheres and Earth System, Key Laboratory of Marine Chemistry Theory and Technology, Ministry of Education, Ocean University of China, Qingdao 266100, China.
E-mail addresses: Lex.Bouwman@pbl.nl (A.F. Bouwman), qzhyao@ouc.edu.cn (Q. Yao).

http://dx.doi.org/10.1016/j.scitotenv.2023.164614
Received 9 February 2023; Received in revised form 8 May 2023; Accepted 31 May 2023
Available online 13 June 2023

1. Introduction

Deoxygenation is the depletion of oxygen in the water column where oxygen consumption exceeds its supply through biological production and air-sea exchange. Deoxygenation has become one of the most important environmental problems in coastal waters in many parts of the world (Breitburg et al., 2018; Carstensen et al., 2014; Oschlies et al., 2018; Rabalais et al., 2014; Wei et al., 2021b). Coastal deoxygenation is driven by decaying organic matter, high water temperature, and water-column stratification (Breitburg et al., 2018). Elevated anthropogenic nutrient discharges enhance oxygen consumption by accelerating oxygen demand from mineralization and decomposition of organic material in the subsurface layer (Chen et al., 2022b; Meng et al., 2022; Oschlies et al., 2018; Reed and Harrison, 2016; Su et al., 2020). Global coastal waters have witnessed an exponential spread of low-oxygen regions in recent decades, partially associated with increased terrestrial N inputs (Conley et al., 2009; Reed and Harrison, 2016). Global riverine nitrogen export fluxes are dominated by agricultural losses (Beusen et al., 2016; Seitzinger et al., 2010; Wang et al., 2020), particularly in rivers with vast areas of agricultural land use such as the Mississippi River (Robertson and Saad, 2021), Yangtze River (Chen et al., 2019; Liu et al., 2018), Yellow River (Wu et al., 2021) and Indus River (Wang et al., 2019b).

Another factor in deoxygenation is water temperature, which controls both oxygen solubility and respiration rate. Climate warming decreases oxygen solubility, enhances stratification, and accelerates oxygen consumption by respiration (Breitburg et al., 2018). Oxygen depletion nowadays exerts widespread and expanding stress on coastal marine ecosystems by reducing biodiversity, affecting biogeochemical cycles and structure and function of coastal ecosystems, and leading to hypoxia or even anoxia (Rabalais et al., 2014).

The relative contributions of water-column oxygen consumption (WOC) and sediment oxygen demand (SOD) vary strongly due to differences in water depth and topography of the seabed (Bourgault et al., 2012; Jørgensen et al., 2022; Meng et al., 2022; Wang et al., 2018b). With drastic changes in nutrient loading and hydrodynamics in coastal waters, understanding the drivers and mechanisms of deoxygenation is crucial to establish comprehensive strategies to control and mitigate deoxygenation and forecast future DO trends.

The Bohai Sea (BS) has been experiencing eutrophication and deoxygenation since 1980s (Wei et al., 2019). The average DO concentrations along a central transect from the Liaohe Estuary to the Yellow River Estuary in the BS showed a declining trend during the period 1976–2014 (Ning et al., 2010; Shi, 2016; Wei et al., 2019; Zhang et al., 2016). The lowest summer bottom oxygen levels in the central BS decreased between 2011 and 2021 and approached the state of hypoxia (Chen et al., 2022b; Zhai et al., 2019). Only one study assessed the contributions of WOC and SOC based on data from coastal waters of the Qinhuangdao (Song et al., 2020) (Fig. 1).

The main research question addressed in this paper is how land-based activities influence deoxygenation through increasing nutrient mobilization. The aims of this study are to (1) quantify the contributions of different oxygen consumption processes in the central Bohai Sea, (2) describe the influence of the main drivers of oxygen consumption including N loading, (3) project the future DO trends using different scenarios for agricultural N use efficiencies. The hydrodynamic D-flow Flexible Mesh module (D-Flow FM), tightly coupled with D-Water Quality module (D-WAQ) from the Delft3D Suite (Deltares, 2022) is used to simulate the oxygen dynamics and relevant hydrodynamic and biochemical processes. Results will help in the development of effective environmental management strategies aimed at mitigating deoxygenation.

2. Materials and methods

2.1. Study area

The BS is a shallow and semi-enclosed inland sea of China (Fig. 1). The weak counter-clockwise gyre comprises the major circulation of the Bohai Sea (Zhou et al., 2017). Due to the limited water exchange with the adjacent northern Yellow Sea, the water residence time in the BS is >1 year (Liu et al., 2017). More than 40 rivers, including the Yellow River, Liao River, Luan River and Hai River, debouch into the BS, which closely link the inland pollution with the water quality and biogeochemistry in the BS. Under the influence of human activities, mainly nutrient losses from agricultural land use, wastewater discharge, and climate change, the BS has been experiencing a series of serious ecological environmental problems during the past four decades, such as eutrophication, frequent occurrence of harmful algal blooms (HABs), deoxygenation and coastal acidification (Wang et al., 2021b; Wei et al., 2019; Xin et al., 2019).

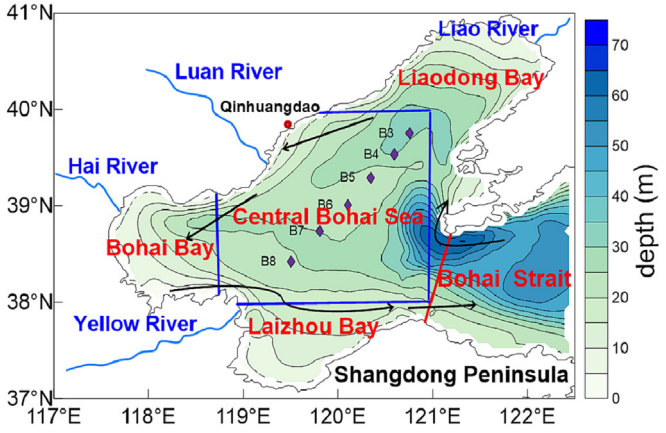

Fig. 1. Location of the study area (central Bohai Sea). The Bohai Sea is geographically divided into the central Bohai Sea, Liaodong Bay, Bohai Bay and Laizhou Bay. The central Bohai Sea covers approximately 41,900 km^2 with an average depth of 24 m. Stations B3-B8 are located in the central transect from the Liaohe Estuary to the Yellow River Estuary of the Bohai Sea.

2.2. Land-based nutrient loading

The Global Nutrient Model (GNM) (Beusen et al., 2015; Beusen et al., 2016; Beusen et al., 2022) was employed to compute river nutrient inputs to the BS for the period 1980–2015 and based on scenarios for the period 2015–2050. IMAGE-GNM is part of the Integrated Model to Assess the Global Environment (IMAGE, version 3.2) (Stehfest et al., 2014). In this framework, IMAGE addresses the societal-ecological links relevant to nutrient sources and eutrophication for the past decades and for the future; GNM describes the complex terrestrial and aquatic biogeochemical processes in the rivers and export to the BS, atmospheric deposition, as well as submarine fresh groundwater discharge (Beusen et al., 2013) and nutrient release from mariculture (Bouwman et al., 2013b). The spatial resolution of IMAGE-GNM is 0.5° × 0.5° (Fig. 2a), and for the river mouths the exact coordinate of the river mouth is used, the location where the data is transferred to the D-Flow FM and D-WAQ modules of the Delft3D Suite (see Section 2.3).

Within the river continuum, IMAGE-GNM describes nutrient delivery to streams, rivers, lakes and reservoirs through diffuse sources via surface runoff and groundwater transport, and nutrient discharge by point sources (Fig. 2a). For every grid cell and every year, the water and nutrient fluxes through streams and rivers, lakes, wetlands and reservoirs (Fig. 2a) are based on the routing scheme, water balance, runoff, discharge and water temperature of the global hydrological model PCR-GLOBWB (Sutanudjaja et al., 2018; Van Beek et al., 2011) (Fig. 2a). In-stream retention in streams, rivers, lakes and reservoirs is calculated in IMAGE-GNM with the nutrient spiraling ecological concept (Newbold et al., 1981; Wollheim et al., 2008). Thus, grid cells receive water and nutrients from upstream water bodies and delivery within the grid cell from diffuse and point sources, and transfer water and nutrients to downstream water bodies in the adjacent grid cell.

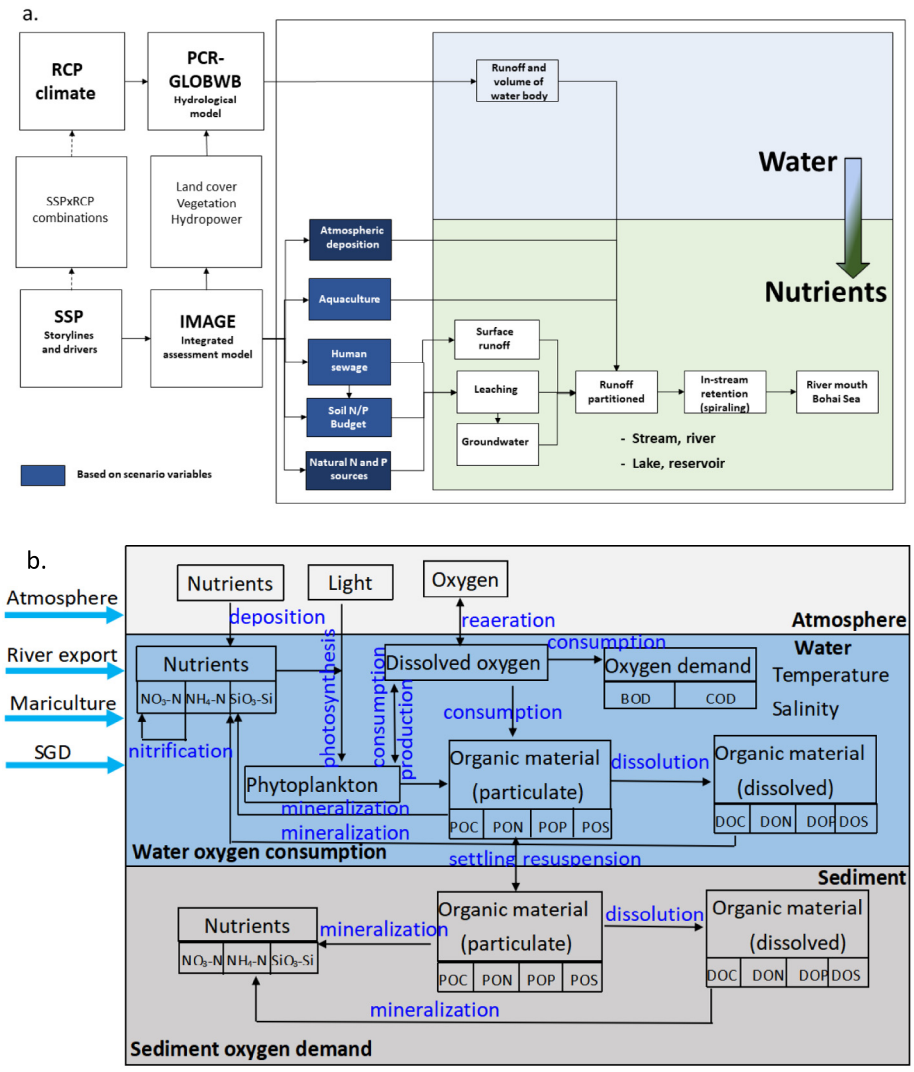

Fig. 2. Scheme of IMAGE-GNM (a); Schematic overview of the D-Water Quality model including state variables, production and consumption processes related to the oxygen (b). BOD, COD, DOC, POC, PON, POP, POS and DOS represent biochemical oxygen demand, chemical oxygen demand, dissolved organic carbon, particulate organic carbon, particulate organic nitrogen, particulate organic phosphorus, particulate organic sulfur and dissolved organic sulfur, respectively.

Due to the large volume of water extraction for irrigation and other purposes, the large number of dams and their management, and the flushing of water and sediment during the water and sediment regulation (since 2002), the hydrology of the Yellow River is not properly simulated by PCR-GLOBWB. Therefore, measured data for the period 1980–2010 on discharge (YRCC, 2010) and nutrient fluxes (Yang et al., 2023) at the mouth of the Yellow River were used instead of the modeled data.

Diffuse sources include N and P delivery from agricultural and natural ecosystems via surface runoff and erosion, outflow of groundwater, groundwater transport through riparian zones to surface water. IMAGE also computes the nutrient release by aquacultural production in freshwater bodies in China (Bouwman et al., 2013a). Natural sources include input of plant litter from vegetation in floodplains and rock weathering (Fig. 2a). The atmospheric N and P deposition data for the BS were obtained from Wang et al. (2020).

The mobilization of nutrients in natural and agricultural ecosystems via these pathways is calculated from surface nutrient budgets, which is the difference between inputs and outputs. In these surface budgets, N and P inputs include (where relevant) animal manure, synthetic fertilizer, biological N fixation and atmospheric deposition. Output or withdrawal is through the harvesting of agricultural crops and grass or forages, or grazing in meadows, ammonia volatilization and denitrification. Natural ecosystems are assumed to be mature, which implies that annual N and P uptake by the vegetation equal the nutrients in litterfall. Since there is no net uptake, inputs from biological N_2 fixation and atmospheric deposition are removed through runoff and erosion, ammonia volatilization, leaching and denitrification.

Point sources include the N and P discharge of rural and urban sewage water from households and industries either directly or after wastewater treatment. Treatment types and their nutrient removal efficiency for China are based on WHO and Unicef (2017). The point sources are described in detail by Van Puijenbroek et al. (2019).

For past agricultural changes we use the data presented recently by Bouwman et al. (2017), while for future changes we use the shared socio-economic pathways (SSP). The five SSPs include a sustainability (SSP1), middle of the road (SSP2), fragmentation (SSP3), inequality (SSP4) and a fossil-fuel based development scenario (SSP5). For each SSP, assumptions and projections were made for domestic production and trade of energy, food, feed and biofuel crops, meat and milk, land use and cover, greenhouse gas emissions and climate change as described earlier by Van Vuuren et al. (2017) and updated for the base year 2015 (Van Vuuren et al., 2021). For each SSP, there is a combination with climate Representative Concentration Pathways (RCP) scenario that is consistent with the climate change projected by each SSP, i.e. SSP1-RCP4.5, SSP2-SSP4 with RCP6.0, and

SSP5-RCP8.5 were implemented (the RCP numbers indicate the projected radiative forcing in W m^{-2} in the year 2100). Assumptions regarding sewage connections and wastewater treatment, agricultural nutrient use efficiencies are consistent with the SSP storylines, with development towards high levels in SSP1 and SSP5, continuation of past trends in SSP2, and mixes of these based on income levels in SSP3 and 4 (for more scenario details see Text S2).

2.3. Marine biogeochemistry

The results of IMAGE-GNM for river export at the location of the river mouth, and simulated submarine groundwater discharge and nutrient release by mariculture and atmospheric deposition are used by the D-Flow FM and D-WAQ modules of the Delft3D Suite, which can be executed independently or in combination (Deltares, 2022). We use the multi-dimensional D-Flow FM module coupled with D-WAQ module (Deltares, 2022). The D-Flow FM model can simulate water flow, waves and currents in river basins, estuaries and coastal waters. The D-WAQ contains a comprehensive set of substances and physical, chemical and ecological processes such as the exchange of substances with the atmosphere, elementary growth of algae and nutrient cycling, nitrification, deposition and resuspension of particles, and adsorption and desorption of contaminant substances (Deltares, 2020). The users can select the processes according to their purpose.

Fig. 2b shows the schematic overview of the D-WAQ including state variables, production and consumption processes related to the oxygen. The main processes involved with oxygen dynamics in the model include air-sea exchange of oxygen (re-aeration) at the air-water interface, oxygen consumption through organic matter decomposition, oxygen consumption through nitrification and primary production (production through photosynthesis/consumption through respiration) in the water column, and organic carbon decomposition in the sediment layer (Fig. 2b), are described in detail in Water Quality Processes Technical Reference Manual (Deltares, 2020). Electron-acceptors (NO_3-N) can engage in the oxidation process, and NO_3-N in the seawater, SGD and mariculture are considered as oxygen sources. Four phytoplankton groups are considered, i.e. diatoms, flagellates, dinoflagellates and Phaeocystis, within each group there are 3 types, i.e. communities sensitive to N, P and light limitation, respectively.

The domain has a curvilinear grid with horizontal resolution of 10 by 10 km with 419 grid cells in the central BS, and 20 sigma layers in vertical direction, with bathymetry derived from the General Bathymetric Chart of the Oceans database. The initial conditions, open boundary, and meteorology applied in the model are presented by Wang et al. (2023). We consider the central BS as a box, and compute the DO input and output fluxes and budget at that level.

Simulations of oxygen production and consumption with a monthly time step cover the period 1980–2010. We focus on the month of August because stratification in August is much stronger than in other months (Zhou et al., 2009). The mean oxygen concentrations in August for the central BS were calculated as the average of the 419 grids. Total dissolved nitrogen (TDN) concentrations were calculated as the sum of the simulated dissolved inorganic nitrogen (DIN) and dissolved organic nitrogen (DON). Total dissolved phosphorus (TDP) concentrations were the sum of the simulated phosphate (PO_4-P) and dissolved organic phosphorus (DOP).

3. Results and discussion

3.1. Comparison with measurement data

The observed DIN riverine export to the BS was 116 Gg/yr during the period 2008–2009 (Liu et al., 2011). Using the ratio of DIN:TN concentration of 0.69 in the Yellow River (Yang et al., 2023), the observation-based estimate of TN river export to the BS was 168 Gg/yr during the years 2008–2009. The IMAGE-GNM modeled export is 254 Gg/yr, but this estimate includes all rivers draining into BS, while the observation-based results include a subset of rivers. The percentage of TN input to the BS due to riverine sources ranged from 29 to 80 % (average 66 %) during the period 1980–2010 (Fig. 4b), which is consistent with previous studies (Wang et al., 2020).

The biogeochemistry model was evaluated with the Root Mean Squared Error (RMSE) (details in Text S1), Pearson's correlation coefficient and bias (Table 1). Results for surface (RMSE = 4 %) and bottom temperature (3 %), surface (9 %) and bottom salinity (9 %), surface DO (4 %), bottom DO (7 %), surface DIN (43 %) and surface PO_4-P (44 %) in the central transect across the BS show good agreement with observations (Fig. 3). The somewhat larger RMSE for DIN and PO_4-P can be partly attributed to the fixed nutrient ratios applied to the various sources to calculate different nutrient forms (see Table S1) (Wang et al., 2023), which may not reflect the actual seasonality of the different sources and nutrient forms.

The significant positive relationships between measured and modeled data except for PO_4-P and surface DO show that their trends are consistent (Table 1). The trend of the salinity was well represented, although the modeled data are slight underestimations (surface ($\delta = -2.65$) and bottom (-2.75) salinity) (Fig. 3c, d), which may be due to low background or initial salinity of the model input.

3.2. N loading

Agricultural sources gradually increased during the period 1980–2010 (Fig. 4a), which was attributed to the rapid increase in fertilizer application and animal manure management. The share of TN delivery to the rivers discharging into the BS from the agricultural sources during 1980–2010 averaged 72 % (60–79 %) (Fig. 4a), which is about the same as the 72 % share of diffuse sources in the TDN inputs to rivers in China in 2012 (Chen et al., 2019). The manure, NO_3-N fertilizers and soil N sources accounted for approximately 55 % of NO_3-N in 30 rivers draining into the Bohai Sea on the basis of NO_3-N dual-isotope ($\delta^{15}N$ and $\delta^{18}O$) (Yu et al., 2021). Similar to the rivers draining into the BS (Fig. 4a), agriculture was also the main source for N delivery to the rivers in the Yangtze River (Chen et al., 2019; Liu et al., 2018), the Mississippi River (Robertson and Saad, 2021), and Indus River (Wang et al., 2019b). The percentage of TN input to the BS due to riverine sources ranged from 29 to 80 % (average 66 %) during the period 1980–2010 (Fig. 4b).

3.3. DO changes

The average modeled DO production by primary production (PP) increased from 1032 Gg in the 1980s to 1140 Gg in the 2000s (Fig. 5a). The water-column oxygen consumption through decomposition (WOC)

Table 1
RMSE (%), Pearson's correlation coefficient (r) and bias (δ) between measured and modeled parameters in August in the central transect from the Liaohe Estuary to the Yellow River Estuary of the Bohai Sea.

	T (°C)		S		DO (μmol/L)		DIN (μmol/L)		PO_4-P (μmol/L)	
	S	B	S	B	S	B	S	B	S	B
RMSE	4	3	9	9	4	7	43	41	44	51
r	0.402*	0.649**	0.832**	0.737**	0.282	0.537**	0.801**	0.825**	0.099	0.009
δ	−0.08	0.15	−2.65	−2.75	2.17	7.89	−1.20	1.25	0.05	0.15

Note: S and B are the abbreviations of surface and bottom, respectively.
** and * indicate correlation is significant at the 0.01 level and 0.05 level, respectively. δ is calculated as the difference in modeled and measured means.

values increased by 20 % from the 1980s to the 2000s (Figs. 5a and S1). The average sediment oxygen demand (SOD) through decomposition and nitrification slightly increased (Figs. 5a and S1). The average air-sea DO flux was minor compared to the PP flux and turned from a small sink in the 1980s (−54 Gg) and 1990s (−10 Gg) to a small source in the 2000s (91 Gg) (Fig. 5a). The contribution of WOC, SOD and nitrification to the total DO consumption during the period 1980–2010 accounted for 61 % on average (range 53–67 %), 11 % (8–13 %) and 14 % (10–17 %), respectively. The results agree with recent experimental data, showing that pelagic respiration and sediment respiration of the west coast of the Bohai Sea in summer 2017 and 2018 were responsible for >60 % and < 40 % (Song et al., 2020). The dominance of WOC in total oxygen consumption in central Bohai Sea is similar to the East China Sea Shelf (Meng et al., 2022), the Changjiang Estuary and adjacent East China Sea (Zhou et al., 2021b), Shiziyang Bay of Southern China (Lai et al., 2022) and the Chesapeake Bay (Li et al., 2016; Su et al., 2020).

Similar to the fluxes of WOC and SOD, the rates of WOC (R_{WOC}) and SOD (R_{SOD}) increased with strong fluctuations during the period 1980–2010 (Fig. 5b, c). R_{WOC} is high in the period April–August (Fig. 5d), while R_{SOD} shows high values in June and July (Fig. 5e). Rising temperatures and increasing amounts of organic material accelerated R_{WOC} (Wang et al., 2018b) and the decomposition of freshly

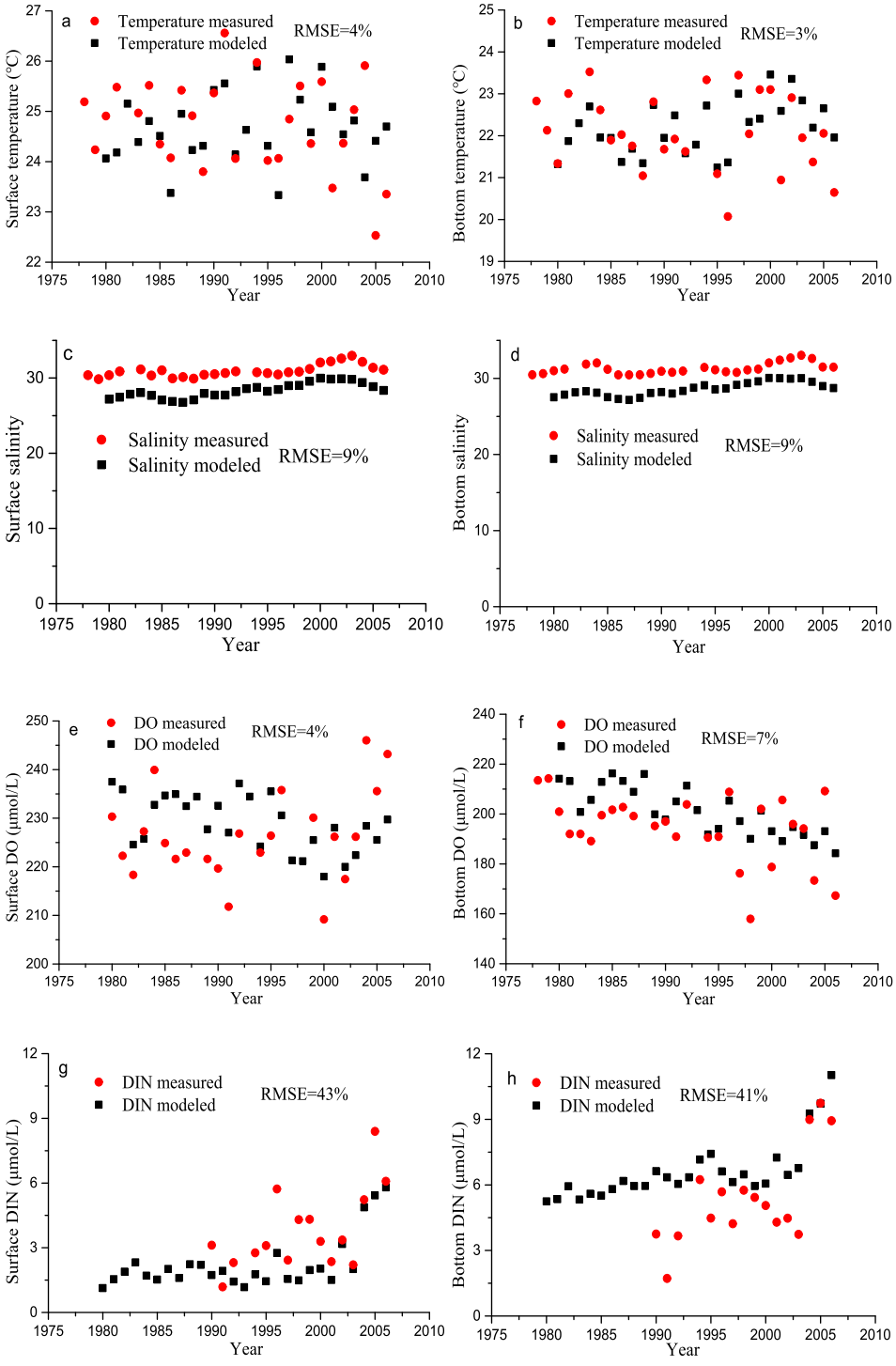

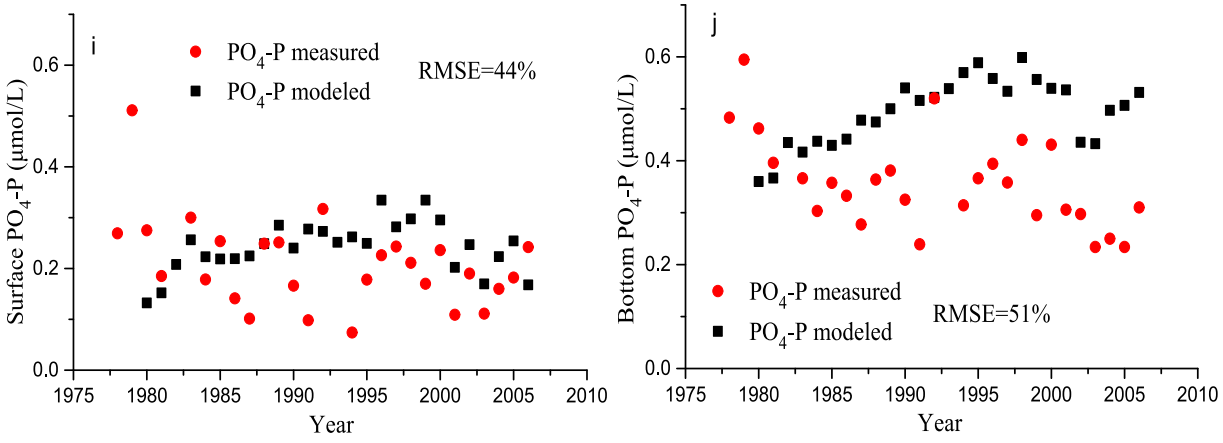

Fig. 3. Comparisons of the observed and modeled surface and bottom temperature (a, b), salinity (c, d), DO (e, f), DIN (g, h) and PO_4-P (i, j) in August in the central transect from the Liaohe Estuary to the Yellow River Estuary of the Bohai Sea. The mean observations of the central transect are from Wang et al. (2019a) and Wei et al. (2019).

deposited organic matter (Carstensen et al., 2014). The R_{WOC} and R_{SOD} were about 1.1–1.6 mmol/(m^3·d) (average 1.2 mmol/(m^3·d)) and 3.5–7.2 mmol/(m^2·d) (average 5.5 mmol/(m^2·d)), respectively (Fig. 5b, c). The simulated aggregated R_{WOC} values were lower than the estimated rates based on observations for the coastal waters of Qinhuangdao city in the northwestern BS with high discharge of sewage (2.13 ± 0.14 mmol/(m^3·d) (average ± standard deviation) in 2011 (Zhai et al., 2012) and 2.18 ± 0.15 mmol/(m^3·d) in 2017 and 2018 (Song et al., 2020). Simulated R_{SOD} were close to the estimated 0.27–10.26 mmol/(m^2·d) with an average of 6.32 ± 2.44 mmol/(m^2·d) based on observations in 2018 (Song et al., 2020). The R_{SOD} in the central BS were similar to those in the Yellow Sea (3.8 mmol/(m^2·d)) and the East China Sea (8.4 mmol/(m^2·d)) (Song et al., 2016) and Baltic Sea (8 mmol/(m^2·d)) (Noffke et al., 2016), and lower than those in the Changjiang Estuary (1.2–25.6 mmol/(m^2·d)) (Cai et al., 2014).

3.4. Nutrient-driven deoxygenation

The differences in temperature between the surface and bottom water (Fig. 6a) and vertical profiles of temperature (Fig. S2a) indicate stratification, which is consistent with Zhou et al. (2009). The surface DO levels with supersaturation clearly exceeded bottom DO (Figs. 6c, d and S2c). Bottom average DO concentrations for 1980–2010, and the minimum and maximum values of the bottom DO during the period 1980–2021 obviously declined at rates of 0.9, 2.1 and 0.9 μmol/L/yr, respectively (Figs. 6c and S3). The thermocline (Fig. S2a) during summer impeded the DO exchange between oxygenated surface water and oxygen-poor bottom water, which enhanced the deoxygenation of bottom waters.

The long water residence time favors the decomposition of organic matter accumulated in water and sediment below the subpycnocline, which causes a reduction of bottom water DO levels (Figs. 6c and S3). The significant positive relationship between Chl-*a* and F_{WOC} shows that eutrophication enhanced WOC, where the decomposed organic matter is mainly from in situ phytoplankton production (Fig. 6g). The stable carbon isotopic composition showed that almost all the organic matter consumed by community respiration in the BS was marine-sourced (Chen et al., 2022b). In contrast, the large amounts of 100–1000 year old recalcitrant terrigenous organic matter supplied by rivers is mostly buried and participates in long-term carbon and nutrient cycles (Zhao et al., 2021).

Parallel to the water column stratification, the surface and bottom TDN, DIN and DON concentrations increased gradually (Figs. 6e and S4a, b), which was attributed to the riverine input, atmospheric deposition, aquaculture and submarine groundwater discharge (Li et al., 2022; Tian et al., 2022; Wang et al., 2019a; Wang et al., 2020; Zhou et al., 2021a). The significant negative relationship between bottom DO and DIN concentrations (Fig. 6h) indicates a strong link between eutrophication and deoxygenation of bottom waters. Nutrient loading is therefore a strong control of WOC in the central BS, causing accelerated WOC and gradual decline of summer bottom DO. Since river export is by far the dominant TN source (Fig. 4b), the river TN export and summer bottom DO also shows a strong negative relationship during 1980–2010 (Fig. 8a, b). Assuming that other conditions (hydrodynamics, climate)

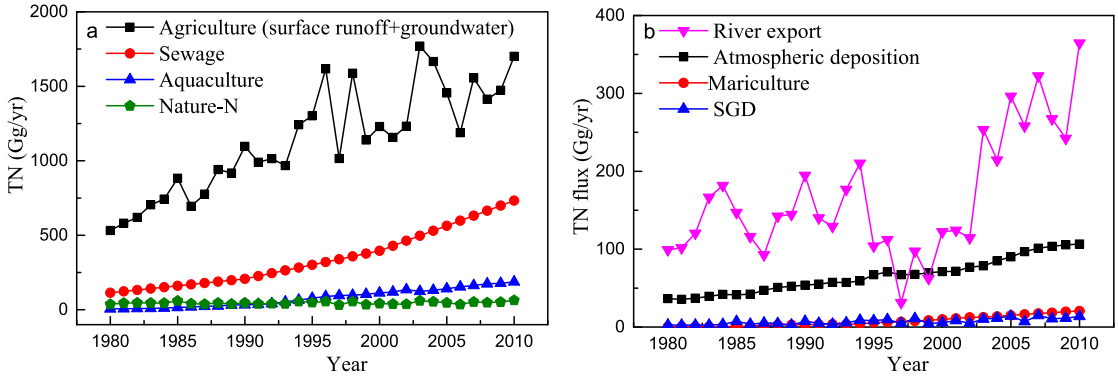

Fig. 4. Simulated contribution of land-based sources of N in the river discharge into the BS (a) and N inputs to the BS from river export, atmospheric deposition, mariculture, and SGD (b) during 1980–2010. The term "Nature-N" is the sum of surface runoff and groundwater in natural areas, and N delivery from vegetation in floodplains and deposition onto surface water.

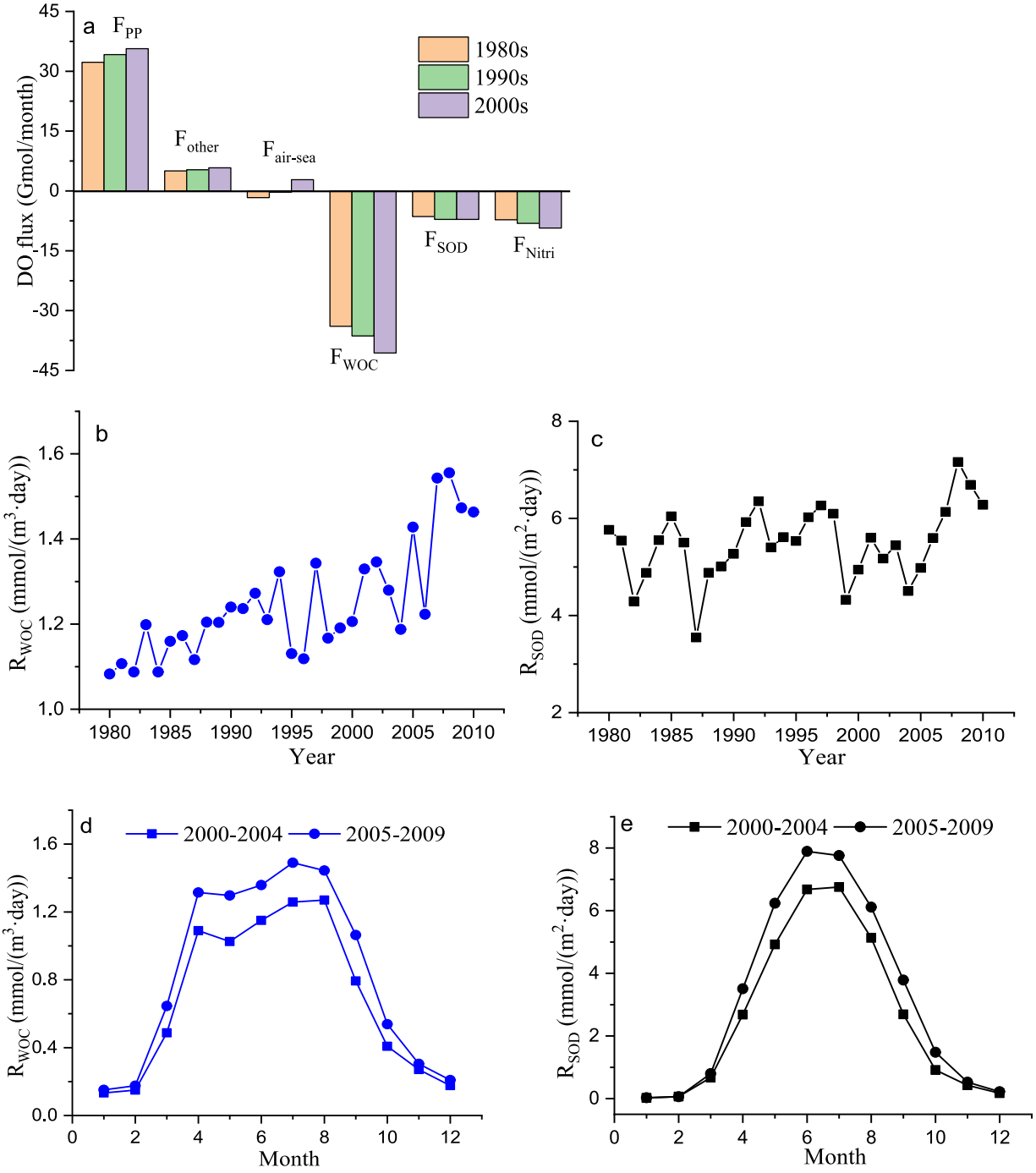

Fig. 5. Average simulated DO fluxes in August for the 1980s, 1990s and 2000s (a), rates of water-column oxygen consumption through decomposition (R_{WOC}) (b) and sediment oxygen demand through decomposition (R_{SOD}) in August during 1980–2010 (c), and the monthly R_{WOC} (d) and R_{SOD} (e) in the central BS. F_{PP}, $F_{air\text{-}sea}$, F_{SOD}, F_{WOC} and F_{nitri} represent the DO input flux from the primary production, the DO exchange between air and sea water, the sediment oxygen demand through decomposition, the water-column oxygen consumption through decomposition and the oxygen consumption through nitrification, respectively. F_{other} is the sum of DO flux from the NO_3-N in the seawater, SGD and mariculture. The positive (+) and negative (−) represents the DO source and sink of the sea water, respectively.

remain equal, we can use projections of future river export TN fluxes to assess future changes in deoxygenation under different scenarios.

3.5. Nutrient imbalances

The disproportionate changes in TDN and TDP concentrations caused imbalances of TDN/TDP ratios in the BS (Figs. 7a and S4e). The TDN/TDP ratios after 2000 exhibited increasing trends to values exceeding the Redfield ratio of 16 (Figs. 7a and S4e), indicating increasing P limitation. While the increasing N availability caused the enhanced primary productivity (Wang et al., 2018a; Wang et al., 2019a; Xin et al., 2019), there is also an increasing nutrient imbalance. This imbalanced nutrient availability caused a gradual shift from a diatom-dominated to a diatom-dinoflagellate dominated or dinoflagellate-dominated system in the BS (Fig. 7b), consistent with previous studies (Chen et al., 2022a; Wang et al., 2019a; Xin et al., 2019).

The significant negative relationship between bottom DO concentrations and dinoflagellate/diatom ratios showed that the dinoflagellate increase accelerated the DO decrease (Fig. 7c). Organic matter associated with dinoflagellates is predominantly decomposed in the water column, because the sinking rates of dinoflagellates are lower than those of diatoms

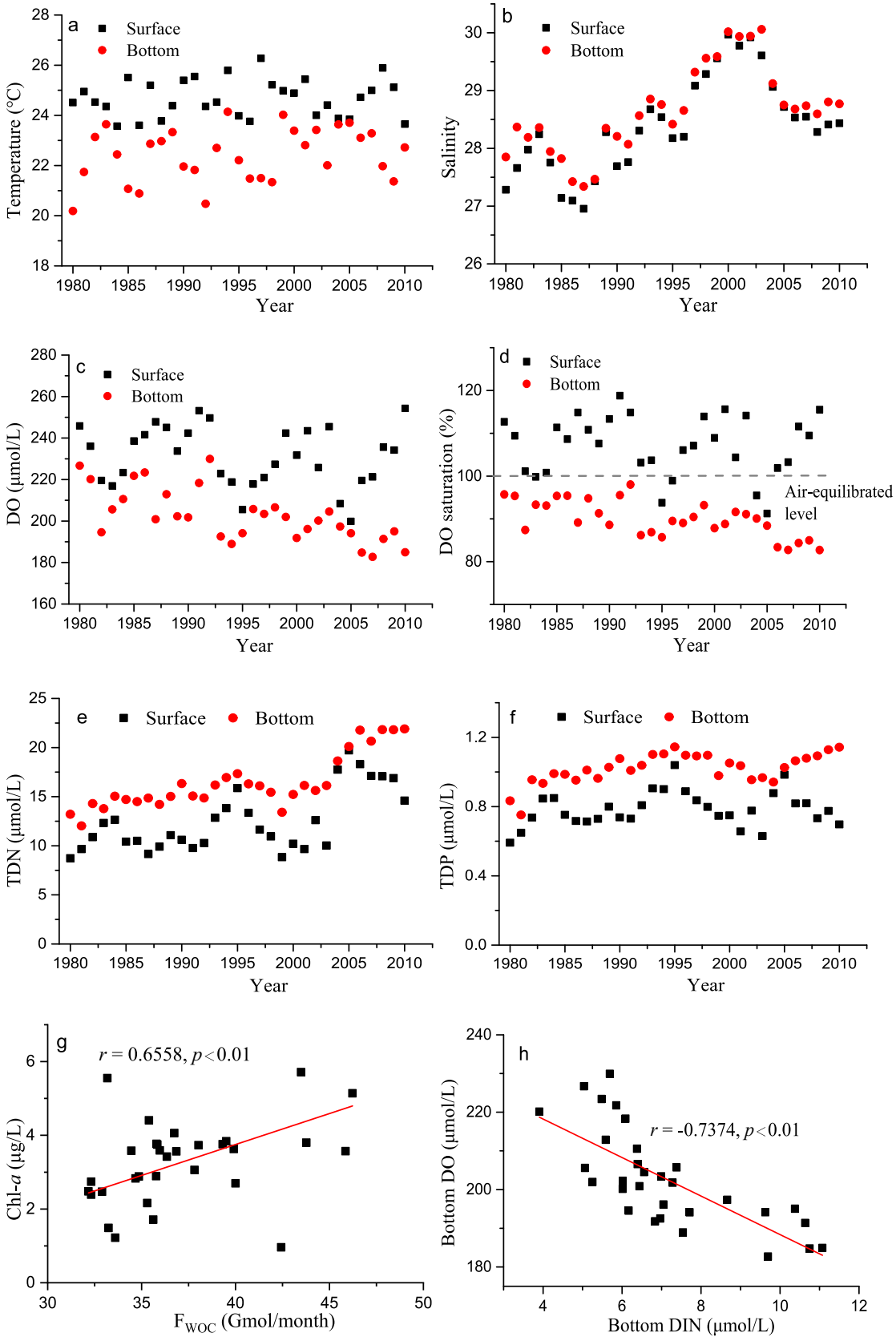

Fig. 6. Simulated average temperature (a), salinity (b), DO concentration (c), DO saturation (d), TDN concentration (e) and TDP concentration (f) for the period 1980–2010, and relationship between Chl-*a* and F_{WOC} (the indirect relationship of the model) (g), and between bottom DO and bottom DIN (h) in August in the central BS.

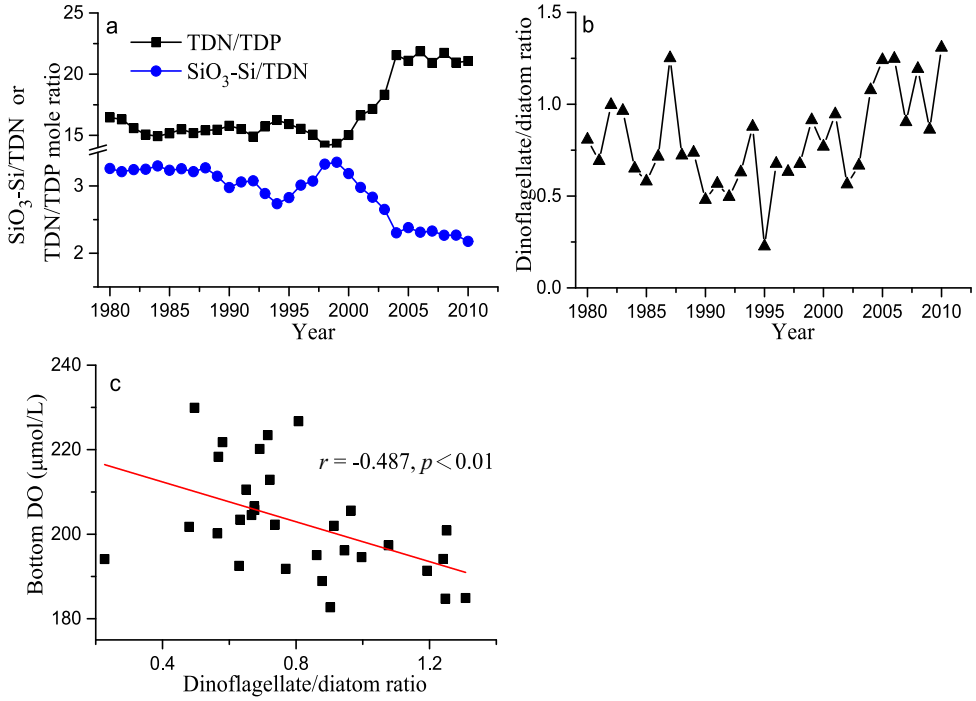

Fig. 7. Annual average molar nutrient ratios (a), and annual ratios of dinoflagellate and diatom (b), and the relationship between bottom DO concentrations and the ratios of dinoflagellate and diatom (c) during the period 1980–2010 in the BS.

(Guo et al., 2014). Wei et al. (2021a) showed that the small-sized dinoflagellate and algae detritus with slow sinking rates enhanced the efficient oxygen consumption in the water column. Furthermore, the increasing DIN concentrations and high N:P ratios were conducive to the proliferation of HABs (Chen et al., 2019; Wang et al., 2021a), which also enhanced deoxygenation (Wei et al., 2019). Therefore, the changes in N:P ratios and resulting deoxygenation are consistent with those observations made by previous work.

3.6. Future risks

Fig. 8 and Fig. S5 show projected river export to the BS according to the five SSPs in 2050. These projections were based on different assumptions for future efficiencies in agriculture and resulting nutrient losses to surface water, different sewage connection rates and wastewater treatment levels, and aquaculture production depending on the storylines of the different SSPs. Compared to 2015, the TN and TP fluxes in rivers discharging into the BS for the five SSPs in 2050 will decline by 26–49 % and 21–55 % (Table S2), with the largest decline in the sustainability oriented SSP1 scenario (with slower increase in agricultural production, less meat consumption, higher efficiency of nutrient use, higher efficiency and improvements in sanitation than in other SSPs). This suggests that deoxygenation may slow down in future decades, especially in the sustainable SSP1 scenario. However, compared to 1980, the TN and TP fluxes in rivers draining into the BS for the five SSPs in 2050 will increase by 121–221 % and 104–259 %, respectively (Table S2). This means that the reductions assumed in SSP1 will not be sufficient to return to the levels prior to 1980.

To improve water quality and ecological environment, the Chinese government launched a series of environmental policies, such as “Zero Growth in Synthetic Fertilizer after 2020” (MOA, 2015), “Action Plan for Prevention and Control of Water Pollution" (GOV, 2015), and “Action Plan for the Uphill Battles for Integrated Bohai Sea Management (2018-2021)” (MEE, 2018). Zero growth of fertilizer use is less optimistic than the assumed 23 % reduction in the SSP1 scenario. Regarding sewage, the TN and TP discharge in wastewater along the coast of the Bohai Sea sharply decreased by approximately 76 % (1.3 to 0.3 Mt) and 89 % (0.16 to 0.02 Mt) from 2015 to 2016, respectively (CSY, 2017), mainly through improved wastewater treatment. This sewage reduction is more than the 32 % assumed in SSP1, but its impact is limited since wastewater is only a small contributor to total nutrient discharge to the BS (Fig. 4).

There are two aspects that may counteract the expected reduction of nutrient loading. Firstly, the legacy from temporarily stored abundant N in soils and groundwater and accumulated P in sediments may release dissolved reactive N and P in future (Beusen et al., 2022; Bouwman et al., 2017; Vilmin et al., 2022) that may not be included in the above projections. A recent example where such legacies counteracted land-based mitigation measures is the Chesapeake Bay, where the hypoxic volume continued to increase, although nutrient loading stabilized or decreased (Li et al., 2016).

Secondly, climate warming is projected to continue in all scenarios (Van Vuuren et al., 2017). Therefore, reduced coastal eutrophication combined with further increasing N/P ratios (Fig. 8) (see also Wang et al., 2021a) and ocean warming in the coming decades may trigger stratification, and consequently HAB proliferation (Sinha et al., 2019; Xiao et al., 2019). In combination with levels of nutrient discharge exceeding those in 1980, there may be a continued risk of bottom water hypoxia in summer in all SSP scenarios in the central BS.

4. Conclusions

Based on modeling for the period 1980–2010, we show that summer bottom DO and minimum bottom DO in the central BS decreased gradually. WOC was the dominant oxygen consumption process (61 %) which increased by 20 % from 1980 to 2010, due to eutrophication and rising temperatures that trigger stratification of the water column. Rivers were by far the dominant source of N loading into BS, and agriculture (average 72 % of the riverine TN in the period 1980–2010) was the dominant contributor to riverine N.

The significant relationship between bottom DO and river N export fluxes was used to project DO trend in future scenarios. Deoxygenation driven by nutrient loading may be reduced in all scenarios, especially the

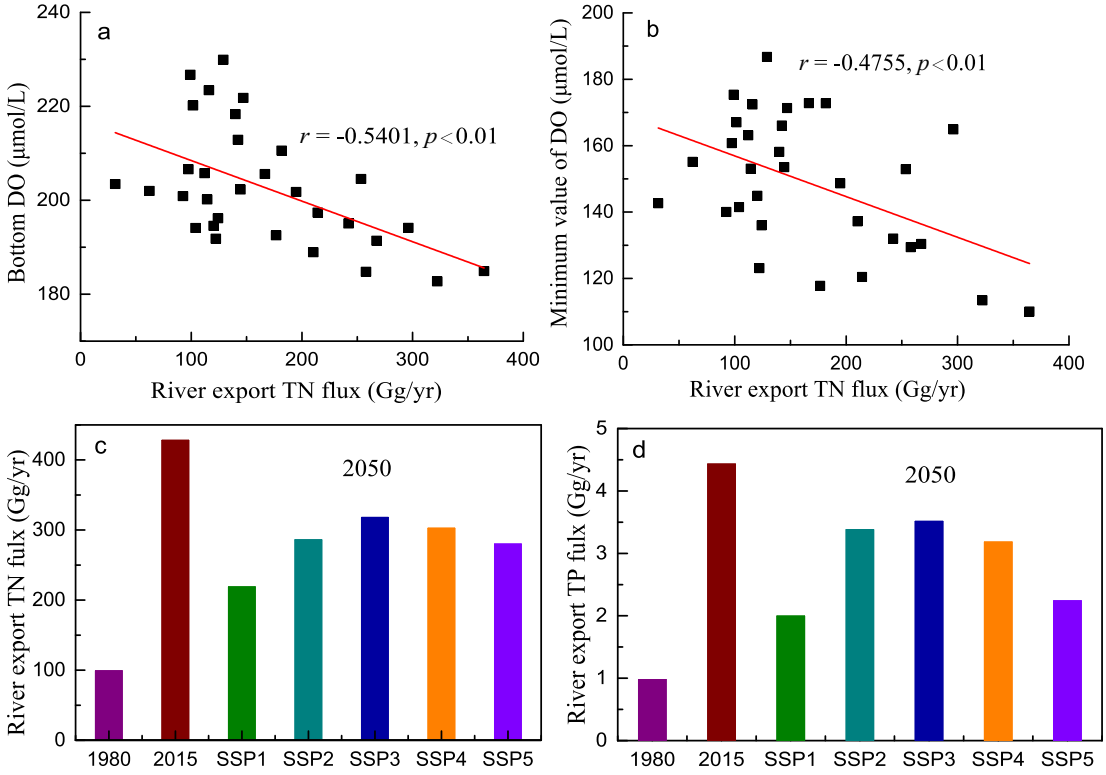

Fig. 8. Relationships between summer bottom DO in the central BS and modeled river export TN flux to the Bohai Sea (a), between minimum value of summer bottom DO and river export TN flux to the Bohai Sea (b) during 1980–2010, and TN (c) and total phosphorus (TP) (d) river export to the Bohai Sea for 1980, 2015, and 2050 for the five SSPs. SSP1, SSP2, SSP3, SSP4 and SSP5 represent the combinations of SSP1-RCP4.5, SSP2-RCP4.5, SSP3-RCP4.5, SSP4-RCP4.5 and SSP5-RCP4.5 scenarios, respectively.

sustainable development scenario with large reduction of river nutrient export. However, the scenarios show that it is difficult to return to N loading and oxygen levels of the 1980s, and that enhanced stratification due to climate warming may still promote summer hypoxia in bottom waters. Nutrient legacies may even counteract the aspired reductions of nutrient loading. A further risk is the continued N:P imbalance, which may cause HAB proliferation. To avoid negative impacts of nutrient loading and imbalances, integrated land-based strategies to manage nutrient releases and transports to coastal ecosystems are needed that account for the nutrient legacies in river basin aquifers and sediments and coastal sediments (Feist et al., 2016; Turner et al., 2008).

CRediT authorship contribution statement

Fuxia Yang: Conceptualization, data analysis, Writing-original draft, review & editing. **Hao Wang:** Ocean biogeochemistry modelling, data analysis, Conceptualization, Writing-review & editing. **Alexander F. Bouwman:** Conceptualization, data analysis, Writing-review & editing. **Arthur Beusen:** Data analysis. **Xiaochen Liu:** Data analysis. **Junjie Wang:** Data analysis. **Zhigang Yu:** Writing-review & editing. **Qingzhen Yao:** Writing-review & editing.

Data availability

Data will be made available on request.

Declaration of competing interest

No conflict of interest exists in the submission of this manuscript, and the manuscript has been approved by all authors for publication. I would like to declare on behalf of my co-authors that the work described was original research that has not been published previously and is not under consideration for publication elsewhere, in whole or in part. All the authors listed have approved the enclosed manuscript.

Acknowledgments

This study was funded by the Joint Fund between NSFC and Shandong Province (U1906210, U22A20580), and the National Natural Science Foundation of China (42130410, 41876116). Fuxia Yang was funded by the China Scholarship Council (grant no. 202106330053).

Appendix A. Supplementary data

Supplementary data to this article can be found online at https://doi.org/10.1016/j.scitotenv.2023.164614.

References

Beusen, A.H.W., Slomp, C.P., Bouwman, A.F., 2013. Global land-ocean linkage: direct inputs of nitrogen to coastal waters via submarine groundwater discharge. Environ. Res. Lett. 8, 034035. https://doi.org/10.1088/1748-9326/8/3/034035.

Beusen, A.H.W., Van Beek, L.P.H., Bouwman, A.F., Mogollón, J.M., Middelburg, J.J., 2015. Coupling global models for hydrology and nutrient loading to simulate nitrogen and phosphorus retention in surface water-description of IMAGE-GNM and analysis of performance. Geosci. Model Dev. 8 (12), 4045–4067. https://doi.org/10.5194/gmd-8-4045-2015.

Beusen, A.H.W., Bouwman, A.F., Van Beek, L.P.H., Mogollón, J.M., Middelburg, J.J., 2016. Global riverine N and P transport to ocean increased during the 20th century despite increased retention along the aquatic continuum. Biogeosciences 13, 2441–2451. https://doi.org/10.5194/bg-13-2441-2016.

Beusen, A.H.W., Doelman, J.C., Van Beek, L.P.H., Van Puijenbroek, P.J.T.M., Mogollón, J.M., Van Grinsven, H.J.M., Stehfest, E., Van Vuuren, D.P., Bouwman, A.F., 2022. Exploring river nitrogen and phosphorus loading and export to global coastal waters in the Shared Socio-economic pathways. Glob. Environ. Chang. 72, 102426. https://doi.org/10.1016/j.gloenvcha.2021.102426.

Bourgault, D., Cyr, F., Galbraith, P.S., Pelletier, E., 2012. Relative importance of pelagic and sediment respiration in causing hypoxia in a deep estuary. J. Geophys. Res.-Oceans 117, C8033. https://doi.org/10.1029/2012jc007902.

Bouwman, A.F., Beusen, A.H.W., Overbeek, C.C., Bureau, D.P., Pawlowski, M., Glibert, P.M., 2013a. Hindcasts and future projections of global inland and coastal nitrogen and phosphorus loads due to finfish aquaculture. Rev. Fish. Sci. 21, 112–156. https://doi.org/10.1080/10641262.2013.790340.

Bouwman, A.F., Beusen, A.H.W., Lassaletta, L., van Apeldoorn, D.F., van Grinsven, H.J.M., Zhang, J., Ittersum Van, M.K., 2017. Lessons from temporal and spatial patterns in global

use of N and P fertilizer on cropland. Sci. Rep.-UK 7 (1). https://doi.org/10.1038/srep40366.
Bouwman, L., Beusen, A., Glibert, P.M., Overbeek, C., Pawlowski, M., Herrera, J., Mulsow, S., Yu, R., Zhou, M., 2013b. Mariculture: significant and expanding cause of coastal nutrient enrichment. Environ. Res. Lett. 8, 044026. https://doi.org/10.1088/1748-9326/8/4/044026.
Breitburg, D., Levin, L.A., Oschlies, A., Grégoire, M., Chavez, F.P., Conley, D.J., Garçon, V., Gilbert, D., Gutiérrez, D., Isensee, K., Jacinto, G.S., Limburg, K.E., Montes, I., Naqvi, S.W.A., Pitcher, G.C., Rabalais, N.N., Roman, M.R., Rose, K.A., Seibel, B.A., Telszewski, M., Yasuhara, M., Zhang, J., 2018. Declining oxygen in the global ocean and coastal waters. Science 359, 1–11. https://doi.org/10.1126/science.aam7240.
Cai, P., Shi, X., Moore, W.S., Peng, S., Wang, G., Dai, M., 2014. ^{224}Ra:^{228}Th disequilibrium in coastal sediments: implications for solute transfer across the sediment-water interface. Geochim. Cosmochim. Ac. 125, 68–84. https://doi.org/10.1016/j.gca.2013.09.029.
Carstensen, J., Andersen, J.H., Gustafsson, B.G., Conley, D.J., 2014. Deoxygenation of the Baltic Sea during the last century. P. Natl. Acad. Sci. 111 (15), 5628–5633. https://doi.org/10.1073/pnas.1323156111.
Chen, K., Li, K., Gao, P., Wang, P., Han, X., Chen, Y., Wang, X., 2022a. Was dissolved nitrogen regime driving diatom to dinoflagellate shift in the Bohai Sea? Evidences from microcosm experiment and modeling reproduction. J. Geophys. Res.-Biogeo. 127, e2021JG006737. https://doi.org/10.1029/2021JG006737.
Chen, X., Strokal, M., Van Vliet, M.T., Stuiver, J., Wang, M., Bai, Z., Ma, L., Kroeze, C., 2019. Multi-scale modeling of nutrient pollution in the rivers of China. Environ. Sci. Technol. 53 (16), 9614–9625. https://doi.org/10.1021/acs.est.8b07352.
Chen, Z., Zhai, W., Yang, S., Zhang, Y., Liu, P., 2022b. Exploring origin of oxygen-consuming organic matter in a newly developed quasi-hypoxic coastal ocean, the Bohai Sea (China): a stable carbon isotope perspective. Sci. Total Environ. 837, 155847. https://doi.org/10.1016/j.scitotenv.2022.155847.
Conley, D., Björck, S., Bonsdorff, E., Carstensen, J., Destouni, G., Gustafsson, B.G., Hietanen, S., Kortekaas, M., Kuosa, H., Meier, H.E.M., Mueller-Karulis, B., Nordberg, K., Norkko, A., Nuernberg, G., Pitkanen, H., Rabalais, N.N., Rosenberg, R., Savchuk, O.P., Slomp, C.P., Zillén, L., 2009. Hypoxia-related processes in the Baltic Sea. Environ. Sci. Technol. 43 (10), 3412–3420. https://doi.org/10.1021/es802762a.
CSY, 2017. National Bureau of Statistics of the People's Republic of China (2015–2017). China Statistical Yearbook (in Chinese). http://www.stats.gov.cn/tjsj/ndsj/.
Deltares, 2020. D-Water Quality User manual. https://www.deltares.nl/en/software/module/d-water-quality/.
Deltares, 2022. D-Flow Flexible Mesh User Manual. Deltares https://www.deltares.nl/en/software/module/d-flow-flexible-mesh/.
Feist, T.J., Pauer, J.J., Melendez, W., Lehrter, J.C., DePetro, P.A., Rygwelski, K.R., Ko, D.S., Kreis, R.G., 2016. Modeling the relative importance of nutrient and carbon loads, boundary fluxes, and sediment fluxes on Gulf of Mexico hypoxia. Environ. Sci. Technol. 50 (16), 8713–8721. https://doi.org/10.1021/acs.est.6b01684.
GOV, 2015. Action Plan for Prevention and Control of Water Pollution. The State Council of the People's Republic of China (in Chinese) https://www.sinosite.com.cn/Public/Admin/202005066581.
Guo, S., Feng, Y., Wang, L., Dai, M., Liu, Z., Bai, Y., Sun, J., 2014. Seasonal variation in the phytoplankton community of a continental-shelf sea: the East China Sea. Mar. Ecol. Prog. Ser. 516, 103–126. https://doi.org/10.3354/meps10952.
Jørgensen, B.B., Wenzhöfer, F., Egger, M., Glud, R.N., 2022. Sediment oxygen consumption: role in the global marine carbon cycle. Earth-Sci. Rev. 228, 103987. https://doi.org/10.1016/j.earscirev.2022.103987.
Lai, Y., Jia, Z., Xie, Z., Li, S., Hu, J., 2022. Water quality changes and shift in mechanisms controlling hypoxia in response to pollutant load reductions: a case study for Shiziyang Bay, Southern China. Sci. Total Environ. 842, 156774. https://doi.org/10.2139/ssrn.4028285.
Li, H., Li, X., Xu, Z., Liang, S., Ding, Y., Song, D., Guo, H., 2022. Nutrient budgets for the Bohai Sea: implication for ratio imbalance of nitrogen to phosphorus input under intense human activities. Mar. Pollut. Bull. 179, 113665. https://doi.org/10.1016/j.marpolbul.2022.113665.
Li, M., Lee, Y.J., Testa, J.M., Li, Y., Ni, W., Kemp, M., Di Toro, D.M., 2016. What drives interannual variability of hypoxia in Chesapeake Bay: climate forcing versus nutrient loading? Geophys. Res. Lett. 43 (5), 2127–2134. https://doi.org/10.1002/2015gl067334.
Liu, J., Du, J., Yi, L., 2017. Ra tracer-based study of submarine groundwater discharge and associated nutrient fluxes into the Bohai Sea, China: a highly human-affected marginal sea. J. Geophys. Res.-Oceans 122 (11), 8646–8660. https://doi.org/10.1002/2017jc013095.
Liu, S., Li, L., Zhang, Z., 2011. Inventory of nutrients in the Bohai. Cont. Shelf Res. 31, 1790–1797. https://doi.org/10.1016/j.csr.2011.08.004.
Liu, X., Beusen, A.H.W., Van Beek, L.P.H., Mogollón, J.M., Ran, X., Bouwman, A.F., 2018. Exploring spatiotemporal changes of the Yangtze River (Changjiang) nitrogen and phosphorus sources, retention and export to the East China Sea and Yellow Sea. Water Res. 142, 246–255. https://doi.org/10.1016/j.watres.2018.06.006.
MEE, 2018. Action Plan for Launching the Tough Battle on the Integrated Rehabilitation of the Bohai Sea (2018–2021). Ministry of Ecological Environment of the People's Republic of China (in Chinese) http://www.gov.cn/gongbao/content/2019/content_5377134.htm (in Chinese).
Meng, Q., Zhang, W., Zhou, F., Liao, Y., Yu, P., Tang, Y., Ma, X., Tian, D., Ding, R., Ni, X., Zeng, D., Schrum, C., 2022. Water oxygen consumption rather than sediment oxygen consumption drives the variation of hypoxia on the East China Sea Shelf. J. Geophys. Res.-Biogeo. 127 (2), e2021J–e6705J. https://doi.org/10.1029/2021jg006705.
MOA, 2015. Plan of Actions Aiming for Zero Arowth in Synthetic Fertilizer Use from 2020 Onwards. Ministry of Agriculture of the People's Republic of China (in Chinese) http://www.zzys.moa.gov.cn/gzdt/201503/t20150318_6309945.htm.
Newbold, J.D., Elwood, J.W., O'Neill, R.V., Winkle, W.V., 1981. Measuring nutrient spiralling in streams. Can. J. Fish. Aquat. Sci. 38, 860–863. https://doi.org/10.1139/f81-114.
Ning, X., Lin, C., Su, J., Liu, C., Hao, Q., Le, F., Tang, Q., 2010. Long-term environmental changes and the responses of the ecosystems in the Bohai Sea during 1960-1996. Deep-Sea Res. II 57 (11−12), 1079–1091. https://doi.org/10.1016/j.dsr2.2010.02.010.
Noffke, A., Sommer, S., Dale, A.W., Hall, P.O.J., Pfannkuche, O., Fry, B., 2016. Benthic nutrient fluxes in the Eastern Gotland Basin (Baltic Sea) with particular focus on microbial mat ecosystems. J. Mar. Syst. 158, 1–12. https://doi.org/10.1016/j.jmarsys.2016.01.007.
Oschlies, A., Brandt, P., Stramma, L., Schmidtko, S., 2018. Drivers and mechanisms of ocean deoxygenation. Nat. Geosci. 11 (7), 467–473. https://doi.org/10.1038/s41561-018-0152-2.
Rabalais, N.N., Cai, W.J., Carstensen, J., Conley, D.J., Fry, B., Hu, X., Quiñones-Rivera, Z., Rosenberg, R., Slomp, C.P., Turner, R.E., Voss, M., Wissel, B., Zhang, J., 2014. Eutrophication-driven deoxygenation in the coastal ocean. Oceanography 27 (1), 172–183. https://doi.org/10.5670/oceanog.2014.21.
Reed, D.C., Harrison, J.A., 2016. Linking nutrient loading and oxygen in the coastal ocean: a new global scale model. Glob. Biogeochem. Cy. 30, 447–459. https://doi.org/10.1002/2015gb005303.
Robertson, D.M., Saad, D.A., 2021. Nitrogen and phosphorus sources and delivery from the Mississippi/Atchafalaya River Basin: an update using 2012 SPARROW Models. J. Am. Water Resour. Assoc. 57 (3), 406–429. https://doi.org/10.1111/1752-1688.12905.
Seitzinger, S.P., Mayorga, E., Bouwman, A.F., Kroeze, C., Beusen, A.H.W., Billen, G., Van Drecht, G., Dumont, E., Fekete, B.M., Garnier, J., Harrison, J.A., 2010. Global river nutrient export: a scenario analysis of past and future trends. Glob. Biogeochem. Cycles 24 (4). https://doi.org/10.1029/2009GB003576.
Shi, Q., 2016. Spatio-temporal mode for inter-annual change of dissolved oxygen and apparentutilization in summer Bohai Sea. J. Appl. Oceanogr. 35 (02), 243–255 (in Chinese with English abstract) https://doi.org/10.3969/J.ISSN.2095-4972.2016.02.014.
Sinha, E., Michalak, A.M., Calvin, K.V., Lawrence, P.J., 2019. Societal decisions about climate mitigation will have dramatic impacts on eutrophication in the 21st century. Nat. Commun. 10 (1), 939. https://doi.org/10.1038/s41467-019-08884-w.
Song, G., Liu, S., Zhu, Z., Zhai, W., Zhu, C., Zhang, J., 2016. Sediment oxygen consumption and benthic organic carbon mineralization on the continental shelves of the East China Sea and the Yellow Sea. Deep-Sea Res. II 124, 53–63. https://doi.org/10.1016/j.dsr2.2015.04.012.
Song, G., Zhao, L., Chai, F., Liu, F., Li, M., Xie, H., 2020. Summertime oxygen depletion and acidification in Bohai Sea, China. Front. Mar. Sci. 7, 252. https://doi.org/10.3389/fmars.2020.00252.
Stehfest, E., Van Vuuren, D.P., Kram, T., Bouwman, A.F., 2014. Integrated Assessment of Global Environmental Change with IMAGE 3.0. Model Description and Policy Applications. PBL Netherlands Environmental Assessment Agency, The Hague.
Su, J., Cai, W.J., Brodeur, J., Hussain, N., Chen, B., Testa, J.M., Scaboo, K.M., Jaisi, D.P., Li, Q., Dai, M., Cornwell, J., 2020. Source partitioning of oxygen-consuming organic matter in the hypoxic zone of the Chesapeake Bay. Limnol. Oceanogr. 65 (8), 1801–1817. https://doi.org/10.1002/lno.11419.
Sutanudjaja, E.H., Van Beek, R., Wanders, N., Wada, Y., Bosmans, J.H.C., Drost, N., Van Der Ent, R.J., De Graaf, I.E.M., Hoch, J.M., De Jong, K., Karssenberg, D., López López, P., Peßenteiner, S., Schmitz, O., Straatsma, M.W., Vannametee, E., Wisser, D., Bierkens, M.F.P., 2018. PCR-GLOBWB 2: a 5 arcmin global hydrological and water resources model. Geosci. Model Dev. 11, 2429–2453. https://doi.org/10.5194/gmd-11-2429-2018.
Tian, S., Gaye, B., Tang, J., Luo, Y., Li, W., Lahajnar, N., Dähnke, K., Sanders, T., Xiong, T., Zhai, W., Emeis, K.C., 2022. A nitrate budget of the Bohai Sea based on an isotope mass balance model. Biogeosciences 19 (9), 2397–2415. https://doi.org/10.5194/bg-19-2397-2022.
Turner, R.E., Rabalais, N.N., Justic, D., 2008. Gulf of Mexico hypoxia: alternate states and a legacy. Environ. Sci. Technol. 42 (7), 2323–2327. https://doi.org/10.1021/es071617k.
Van Beek, L.P.H., Wada, Y., Bierkens, M.F.P., 2011. Global monthly water stress: 1. Water balance and water availability. Water Resour. Res. 47 (7), W7517. https://doi.org/10.1029/2010wr009791.
Van Puijenbroek, P.J.T.M., Beusen, A.H.W., Bouwman, A.F., 2019. Global nitrogen and phosphorus in urban waste water based on the Shared Socio-economic pathways. J. Environ. Manag. 231, 446–456. https://doi.org/10.1016/j.jenvman.2018.10.048.
Van Vuuren, D., Stehfest, E., Gernaat, D., De Boer, H.S., Daioglou, V., Doelman, J., Edelenbosch, O., Harmsen, J.H.M., van Zeist, W.J., Van den Berg, M., Dafnomilis, I., Sluisveld, M., Tabeau, A., Vos, L., Waal, L., Berg, N., Beusen, A., Bos, A., Biemans, H., Castillo, V., 2021. The 2021 SSP Scenarios of the IMAGE 3.2 Model.
Van Vuuren, D.P., Stehfest, E., Gernaat, D.E.H.J., Doelman, J.C., van den Berg, M., Harmsen, M., de Boer, H.S., Bouwman, L.F., Daioglou, V., Edelenbosch, O.Y., Girod, B., Kram, T., Lassaletta, L., Lucas, P.L., van Meijl, H., Müller, C., van Ruijven, B.J., van der Sluis, S., Tabeau, A., 2017. Energy, land-use and greenhouse gas emissions trajectories under a green growth paradigm. Glob. Environ. Chang. 42, 237–250. https://doi.org/10.1016/j.gloenvcha.2016.05.008.
Vilmin, L., Bouwman, A.F., Beusen, A.H.W., van Hoek, W.J., Mogollón, J.M., 2022. Past anthropogenic activities offset dissolved inorganic phosphorus retention in the Mississippi River basin. Biogeochemistry 161 (2), 157–169. https://doi.org/10.1007/s10533-022-00973-1.
Wang, B., Xin, M., Wei, Q., Xie, L., 2018a. A historical overview of coastal eutrophication in the China Seas. Mar. Pollut. Bull. 136, 394–400. https://doi.org/10.1016/j.marpolbul.2018.09.044.
Wang, H., Hu, X., Wetz, M.S., Hayes, K.C., 2018b. Oxygen consumption and organic matter remineralization in two subtropical, eutrophic coastal embayments. Environ. Sci. Technol. 52 (22), 13004–13014. https://doi.org/10.1021/acs.est.8b02971.
Wang, H., Bouwman, A.F., Van Gils, J., Vilmin, L., Beusen, A., Wang, J., Liu, X., Yu, Z., Ran, X., 2023. Hindcasting HAB risk under impacts of land-based nutrient pollution in the Eastern Chinese coastal Seas. Water Res. 231, 119669. https://doi.org/10.1016/j.watres.2023.119669.
Wang, J., Yu, Z., Wei, Q., Yao, Q., 2019a. Long-term nutrient variations in the Bohai Sea over the past 40 years. J. Geophys. Res.-Oceans 124 (1), 703–722. https://doi.org/10.1029/2018jc014765.
Wang, J., Beusen, A.H.W., Liu, X., Van Dingenen, R., Dentener, F., Yao, Q., Xu, B., Ran, X., Yu, Z., Bouwman, A.F., 2020. Spatially explicit inventory of sources of nitrogen inputs to the

Yellow Sea, East China Sea, and South China Sea for the period 1970-2010. Earth's Future 8 (10), e1516E–e2020E. https://doi.org/10.1029/2020ef001516.

Wang, J., Bouwman, A.F., Liu, X., Beusen, A.H.W., Van Dingenen, R., Dentener, F., Yao, Y., Glibert, P.M., Ran, X., Yao, Q., Xu, B., Yu, R., Middelburg, J.J., Yu, Z., 2021a. Harmful Algal Blooms in Chinese coastal waters will persist due to perturbed nutrient ratios. Environ. Sci. Technol. Lett. 8 (3), 276–284. https://doi.org/10.1021/acs.estlett.1c00012.

Wang, M., Tang, T., Burek, P., Havlík, P., Krisztin, T., Kroeze, C., Leclère, D., Strokal, M., Wada, Y., Wang, Y., Langan, S., 2019b. Increasing nitrogen export to sea: a scenario analysis for the Indus River. Sci. Total Environ. 694, 133629. https://doi.org/10.1016/j.scitotenv.2019.133629.

Wang, Y., Liu, D., Xiao, W., Zhou, P., Tian, C., Zhang, C., Jinzhou, Du, Guo, H., Wang, B., 2021b. Coastal eutrophication in China: trend, sources, and ecological effects. Harmful Algae 107, 102058. https://doi.org/10.1016/j.hal.2021.102058.

Wei, H., Zhao, L., Zhang, H., Lu, Y., Yang, W., Song, G., 2021a. Summer hypoxia in Bohai Sea caused by changes in phytoplankton community. Anthropocene Coasts 4 (1), 77–86. https://doi.org/10.1139/anc-2020-0017.

Wei, Q., Wang, B., Yao, Q., Xue, L., Sun, J., Xin, M., Yu, Z., 2019. Spatiotemporal variations in the summer hypoxia in the Bohai Sea (China) and controlling mechanisms. Mar. Pollut. Bull. 138, 125–134. https://doi.org/10.1016/j.marpolbul.2018.11.041.

Wei, Q., Xue, L., Yao, Q., Wang, B., Yu, Z., 2021b. Oxygen decline in a temperate marginal sea: contribution of warming and eutrophication. Sci. Total Environ. 757, 143227. https://doi.org/10.1016/j.scitotenv.2020.143227.

WHO, Unicef, 2017. Joint Monitoring Programme for Water Supply, Sanitation and Hygiene. Estimates on the Use of Water, Sanitation and Hygriene by Country (2000-2015).

Wollheim, W., Vörösmarty, C.J., Bouwman, A.F., Green, P., Harrison, J., Meybeck, M., Peterson, B.J., Seitzinger, S.P., Syvitski, J., 2008. Global N removal by freshwater aquatic systems using a spatially distributed, within-basin approach. Glob. Biogeochem. Cycles 22. https://doi.org/10.1029/2007GB002963.

Wu, N., Liu, S.M., Zhang, G.L., Zhang, H.M., 2021. Anthropogenic impacts on nutrient variability in the lower Yellow River. Sci. Total Environ. 755, 142488. https://doi.org/10.1016/j.scitotenv.2020.142488.

Xiao, X., Agustí, S., Pan, Y., Yu, Y., Li, K., Wu, J., Duarte, C.M., 2019. Warming amplifies the frequency of Harmful Algal Blooms with eutrophication in Chinese coastal waters. Environ. Sci. Technol. 53 (22), 13031–13041. https://doi.org/10.1021/acs.est.9b03726.

Xin, M., Wang, B., Xie, L., Sun, X., Wei, Q., Liang, S., Chen, K., 2019. Long-term changes in nutrient regimes and their ecological effects in the Bohai Sea, China. Mar. Pollut. Bull. 146, 562–573. https://doi.org/10.1016/j.marpolbul.2019.07.011.

Yang, F.X., Yu, Z.G., Bouwman, A.F., Chen, H.T., Jian, H.M., Beusen, A.H.W., Liu, X.C., Yao, Q.Z., 2023. Human-driven long-term disconnect of nutrient inputs to the Yellow River basin and river export to the Bohai Sea. J. Hydrodyn. 618, 129279. https://doi.org/10.1016/j.jhydrol.2023.129279.

YRCC, 2010. Yellow River Conservancy Commission. http://www.yrcc.gov.cn/.

Yu, J., Zhang, W., Tan, Y., Zong, Z., Hao, Q., Tian, C., Zhang, H., Li, J., Fang, Y., Zhang, G., 2021. Dual-isotope-based source apportionment of nitrate in 30 rivers draining into the Bohai Sea, north China. Environ. Pollut. 283, 117112. https://doi.org/10.1016/j.envpol.2021.117112.

Zhai, W., Zhao, H., Zheng, N., Xu, Y., 2012. Coastal acidification in summer bottom oxygen-depleted waters in northwestern-northern Bohai Sea from June to August in 2011. Chin. Sci. Bull. 57 (9), 1062–1068. https://doi.org/10.1007/s11434-011-4949-2.

Zhai, W.D., Zhao, H.D., Su, J.L., Liu, P.F., Li, Y.W., Zheng, N., 2019. Emergence of summertime hypoxia and concurrent carbonate mineral suppression in the central Bohai Sea, China. J. Geophys. Res.-Biogeo. 124 (9), 2768–2785. https://doi.org/10.1029/2019jg005120.

Zhang, H., Li, Y.F., Tang, C., Zou, T., Yu, J., Guo, K., 2016. Spatial characteristics and formation mechanisms of bottom hypoxia zone in the Bohai Sea during summer. Chin. Sci. Bull. 61 (14), 1612–1620 (in Chinese with English abstract) https://doi.org/10.1360/n972015-00915.

Zhao, B., Yao, P., Bianchi, T.S., Yu, Z.G., 2021. Controls on organic carbon burial in the Eastern China Marginal Seas: a regional synthesis. Glob. Biogeochem. Cy. 35, e2020G–e6608G. https://doi.org/10.1029/2020gb006608.

Zhou, D., Yu, M., Yu, J., Li, Y., Guan, B., Wang, X., Wang, Z., Lv, Z., Qu, F., Yang, J., 2021a. Impacts of inland pollution input on coastal water quality of the Bohai Sea. Sci. Total Environ. 765, 142691. https://doi.org/10.1016/j.scitotenv.2020.142691.

Zhou, F., Huang, D., Su, J., 2009. Numerical simulation of the dual-core structure of the Bohai Sea cold bottom water in summer. Chin. Sci. Bull. 54 (23), 4520–4528. https://doi.org/10.1007/s11434-009-0019-4.

Zhou, F., Huang, D.J., Xue, H.J., Xuan, J.L., Yan, T., Ni, X.B., Zeng, D.Y., Li, J., 2017. Circulations associated with cold pools in the Bohai Sea on the Chinese continental shelf. Cont. Shelf Res. 137, 25–38. https://doi.org/10.1016/j.csr.2017.02.005.

Zhou, J., Zhu, Z., Hu, H., Zhang, G., Wang, Q., 2021b. Clarifying Water Column Respiration and Sedimentary Oxygen Respiration under oxygen depletion off the Changjiang Estuary and adjacent East China Sea. Front. Mar. Sci. 7, 623581. https://doi.org/10.3389/fmars.2020.623581.